

# Fluorescence Probes for Cyclodextrin Interiors

Khader A. Al-Hassan<sup>1</sup> and Mohammad F. Khanfer<sup>1</sup>

Received October 27, 1997; accepted April 27, 1998

6-Propionyl-2-(dimethylamino)naphthalene (PRODAN) emits two fluorescence bands, at  $\sim 510$  and  $\sim 435$  nm, when dissolved in  $\gamma$ -cyclodextrin (CD) aqueous solutions. The relative contributions of these two bands were found to depend on time and temperature. These emissions are attributed to the inclusion of PRODAN with the dimethylamino group toward the larger and smaller rims inside the  $\gamma$ -CD cavities, respectively. The first position corresponds to a slightly polar and slightly rigid environment, while the second corresponds to a hydrophobic and rigid environment relative to the aqueous polar bulk. In contrast, PRODAN in either  $\alpha$ -CD or  $\beta$ -CD aqueous solutions emits a single fluorescence band at 525 and 510 nm, respectively. The emission of PRODAN in  $\alpha$ -CD is similar to that in water and indicates no inclusion at all. In  $\beta$ -CD, only one kind of inclusion is possible with the dimethylamino group of PRODAN toward the larger rims of  $\beta$ -cavities. These results are supported by fluorescence decay lifetime measurements and are consistent with our previous observations made for 4-dimethylaminobenzonitrile (DMABN) and 4-diethylaminobenzonitrile (DEABN) in  $\alpha$ - and  $\beta$ -CD aqueous solutions [23,24]. Therefore the possibility of twisted intramolecular charge transfer (TICT) state formation in PRODAN in terms of environmental polarity and local free volume of CD cavities is discussed. These observations put PRODAN, DMABN, and other TICT compounds as fluorescence probes for CD interiors.

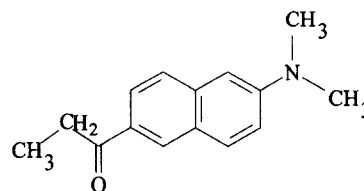
**KEY WORDS:** PRODAN; cyclodextrins; twisted intramolecular charge transfer; local polarity; microenvironmental viscosity.

## INTRODUCTION

6-Propionyl-2-(*N,N*-dimethylamino)naphthalene (PRODAN), an organic molecule designed by Weber *et al.* [1] during 1979 as a biological probe, was found to undergo large changes in its fluorescence properties in solvents of various polarities [1–5] (Scheme I). It shows a broad fluorescence band with a clear red shift upon increasing the solvent polarity. For example the emission maximum is red shifted from  $\sim 400$  nm in cyclohexane to  $\sim 530$  nm in water, which indicates a dipole moment enhancement upon electronic transition to the first excited state. For PRODAN, and according to Lippert theory [1], the dipole moment of the first singlet excited

state was estimated to be around 20D. [1], which is quite large in comparison to those of other fluorophores. Hence, PRODAN was employed extensively as a probe of local polarity in various biological environments such as protein interiors, membranes, and lipid bilayers [6–10].

In these systems, the fluorescence properties of PRODAN were found to undergo appreciable changes



Scheme I. PRODAN.

<sup>1</sup> Department of Chemistry, Yarmouk University, Irbid, Jordan. Fax: 962-2-247983 or 274725.

[6–10], mainly the appearance of two local maxima in the fluorescence emission, one at  $\sim 435$  nm and the other at  $\sim 510$  nm representing emissions from less polar and more polar excited states, respectively. The relative contributions and the exact positions of these two fluorescence bands depend on the local polarity and microenvironmental viscosity of the medium under study.

For example, Chong [6] has studied the effect of pressure elevation on the location of PRODAN in various membrane lipids (which are composed of a polar water–lipid interface and a relatively less polar hydrocarbon cone) and found PRODAN to exhibit two fluorescence maxima, at  $\sim 435$  and  $\sim 530$  nm. The 435-nm fluorescence band was found to be enhanced relative to the 530-nm band upon pressure elevation and was attributed to relocation of PRODAN from the polar water–lipid interface to the less polar hydrocarbon cone and to the solvent relaxation, which becomes slower upon pressure enhancement. This conclusion was utilized by Sommer *et al.* [7] to study molecular dynamics of the surface of membranes composed of ether or ester derivatives of various choline glycerophospholipids. The lifetimes and the fluorescence spectra measurements made on PRODAN in these lipids revealed that solvent relaxation in ether lipid bilayers is faster than in diacyl lipid membranes. Moreover, Zeng and Chong [8] used PRODAN fluorescence as a probe to study the interactions between pressure and ethanol on the formation of interdigitated dipalmitoylphosphatidylcholine (DPPC) liposomes. An increase in either ethanol concentration or pressure lead to a red shift and enhancement of the 510-nm relative to the 435-nm fluorescence band. These variations were correlated to PRODAN relocation from a less polar to a more polar environment as a result of lipid interdigitation.

Rottenberg [9] studied the emission spectra of PRODAN in red blood cell ghosts and observed a peak at  $\sim 505$  nm and a shoulder at  $\sim 435$  nm which vary in their intensity as a function of temperature. In another study of chemical interest Narang *et al.* [10] used the steady fluorescence of PRODAN to probe the gelation process of the widely used tetramethylorthosilicate-derived sol-gels. The red shift of the fluorescence of PRODAN, which was followed by a blue shift, was attributed to expulsion of ethanol molecules first (water content will be larger and hence more polar), followed by removal of water molecules. They attributed the enhancement of the 435 nm (which becomes a peak) upon lowering the temperature to  $\sim 5^\circ\text{C}$  to the existence of a nonrelaxed state (rigid local environment) and/or to binding of PRODAN to a less polar site.

Since PRODAN has a structural feature similar to that possessed by 4-dimethylaminobenzonitrile (DMABN) in the sense that it has a dimethylamino group as donor and a propionyl group as acceptor, it may have the potential to transform to a twisted intramolecular charge transfer (TICT) state during the excited-state lifetime in a manner similar to that exhibited by DMABN and emit TICT fluorescence besides the normal fluorescence band.

A few decades ago, Lippert [11] reported that DMABN shows a single fluorescence band at about 360 nm in nonpolar solvents. In polar solvents, an additional band appears, which resides in the 450- to 500-nm range. The shorter-wavelength band is usually observed in the fluorescence emission of benzene derivatives and is usually named the normal or B-band. The additional fluorescence feature was attributed to the charge transfer action mentioned above and is usually named the anomalous or A-band.

Lippert *et al.* [11] have employed Platt's notation to assign the states responsible for the normal and anomalous emissions. They originally proposed that there are two excited states, a highly polar  ${}^1L_a$  and a relatively nonpolar  ${}^1L_b$  state, responsible for the anomalous and normal emissions, respectively.

Fluorescence polarization measurements for the alkoxy carbonyl derivatives of DMABN in glycerol carried out by Wermuth and Rettig [12] showed that both the A- and the B-bands originate from the  ${}^1L_a$ -state with no level reversal, indicating that the proposal of Lippert *et al.* is valid for the case of DMABN, but ruled out for other molecules that exhibit similar dual fluorescence.

The demand for a more general explanation for the dual fluorescence was satisfied by Grabowski *et al.* [13], who were the first to introduce the concept of TICT to the field of excited-state processes. They suggested that the TICT state is created as a result of twisting of the donor group to an approximately perpendicular configuration, followed by an intramolecular charge transfer and then a solvent relaxation around the generated TICT state. So emission from the TICT state appears as the observed anomalous band.

For the case of PRODAN, the presence of the dimethylamino group (donor) at position 2 and the propionyl substituent at position 6, on the opposite edges of the naphthalene moiety, invited researchers to seek for the possibility of fluorescence from the TICT-emitting state of PRODAN.

In this direction, Rollinson and Drickamer [14] have assumed a model of two excited states (locally excited and charge transfer) in PRODAN, in analogy to para-(9-anthryl)dimethylaniline (ADMA), a compound

showing fluorescence from a pure TICT state. But the results obtained from their comparative, high-pressure study and the fluorescence lifetime measurements failed to confirm the presence of charge transfer state according to the assumed model. On the other hand, Lackowics and Balter [5] have employed fluorescence phase and modulation methods to study the fluorescence emission of PRODAN in *n*-butanol at 218 K. The results obtained confirmed that solvent relaxation involves at least two steps and, hence, an excited-state process exists.

A theoretical approach to the argument was carried out by Nowak *et al.* [4]. Their theoretical calculations assume that only the conformer with a twisted dimethylamino group has an excited-state dipole moment high enough to explain the spectral properties of PRODAN, at least in polar solvents.

More theoretical support for the presence of a TICT state in PRODAN was obtained from a semiempirical molecular orbital study carried out by Ilich and Prendergast [15]. The evaluated data predict that generation of the excited singlet state occurs as a result of two processes: deformation of the ring, followed by a charge transfer from the nitrogen atom to the rest of the molecule.

Experimental evidence supporting the theoretical approaches mentioned above was provided by Heisel *et al.* [16]. They have studied steady-state and normalized instant fluorescence emission of PRODAN in *n*-butanol at low temperatures. The corrected steady-state fluorescence undergo both a blue shift and broadening upon temperature depression in the range  $-24$  to  $-75^{\circ}\text{C}$ . The instant spectrum at  $-75^{\circ}\text{C}$  was red shifted with time from 0.25 to 15 ns after excitation. The obtained blue shift and broadening were explained by the presence of two superimposable emitting states, one being the precursor to the other, with an intramolecular reaction rate depending on the temperature so that the contribution of the higher-energy emitting state increases as temperature decreases. The red shift obtained in the instant spectra is attributed to polar solvent relaxation around the excited dipole moment. These results led Heisel *et al.* [16] to assume the presence of an excited-state intramolecular reaction, accompanied by a solvent relaxation.

An argument that stands beside all the theoretical and empirical support for the existence of a TICT state on excited PRODAN molecules is that of Bunker *et al.* [17]. They suggested that the behavior of PRODAN does not follow a classical TICT-state formation mechanism, however the character of the excited state could still be similar to that of a TICT state. The fact that PRODAN fluorescence emission undergoes nearly the same solvatochromic shifts as the TICT fluorescence of

*p*-(*N,N*-diethylamino)ethylbenzoate (DEAEB) led them to believe that the emitting excited state of PRODAN has the same character as a charge transfer emitting state, though somewhat different from a classical TICT state.

The TICT phenomenon mentioned above has two significant properties. First, it is a dynamical process that involves twisting of the donor group, and therefore it can probe local microviscosity; second, it is a charge-separation process and, hence, is sensitive to environmental polarity [18]. So these properties invited researchers to utilize the TICT phenomenon to probe media of appreciable viscosities and polarities, such as polymers [19–22] and cyclodextrins [23–25].

Cyclodextrins are cyclic oligosaccharides that possess hydrophobic cavities which can encapsulate organic and organometallic molecules in aqueous solutions [26–29]. The geometry of the cyclodextrin gives it the shape of a cone. Three types of cyclodextrins are commonly available, each having a slightly different cavity diameter:  $\alpha$ -CD, with a 5.7-Å cavity;  $\beta$ -CD, with a 7.8-Å cavity; and  $\gamma$ -CD, with a 9.5-Å cavity. The variable cavity diameter of the cyclodextrins has been used to encapsulate molecules based on their size. The interior of the cavity constitutes a relatively hydrophobic environment which affects the emission of the solute molecules. The restricted shape and size of the cavity geometrically constrain the solute molecule and, therefore, markedly affect its properties [23,24].

Since the TICT formation process involves both twisting of the donor moiety and charge-separation processes, it can investigate cyclodextrin environments, and vice versa.

In this context, Al-Hassan and co-workers [23] have reported the fluorescence of DMABN dissolved in an aqueous solution of  $\alpha$ -CD. The collected results suggest that the probe (DMABN) exists in three different environmental conditions, namely, the probe in the aqueous bulk, where DMABN is surrounded by water molecules representing the most polar and least rigid environment; DMABN inside the  $\alpha$ -CD cavity with the dimethylamino group directed toward the larger rim of the cavity, representing a slightly rigid and slightly polar environment; and DMABN inside the  $\alpha$ -cavity with the dimethylamino group directed toward the smaller rim of the cavity, representing the least polar and most rigid environment. One of the most significant features of this work is the role of the rotating moiety, the dimethylamino group, which is believed to control the mechanism of inclusion. The role of the rotating group was confirmed by extension of this study to include the spectral behavior of *p*-(*N,N*-diethylamino)benzotrile (DEABN) in  $\alpha$ -CD aqueous solutions [24]. The diethylamino group

is bigger than the dimethylamino group, and it is probably interlocked in the hydrophobic environment and, as a consequence, is unable to rotate during the excited state lifetime. Actually this was concluded from the experimental observation that the TICT band around 460 nm is present in the case of DMABN and is absent in the case of DEABN, confirming the role of the rotating group in determination the excited-state characteristics of the probes mentioned above in  $\alpha$ -CD aqueous solutions.

The purpose of the present work was to investigate the role of the twisting moiety, the dimethylamino group, in the creation of the emitting state(s) in excited PRODAN molecules. This aim can be accomplished by inviting the fluorescence spectral properties of PRODAN in  $\alpha$ -,  $\beta$ -, and  $\gamma$ -CD aqueous solutions. Here, no appreciable effects in  $\alpha$ -CD, a small effect in  $\beta$ -CD; and dramatic changes in  $\gamma$ -CD were observed.

## EXPERIMENTAL

### Preparation of PRODAN Cyclodextrin Aqueous Solutions

PRODAN from Molecular Probes Inc. (Eugene, OR) was used as supplied.  $\alpha$ -,  $\beta$ -, and  $\gamma$ -CD (Wako Pure Products) were kindly supplied by Professor T. Azumi (Tohoku University, Sendi) and were used without further purification. Water was doubly distilled, deionized. Its purity was checked by obtaining the absorption spectrum.

A stock aqueous solution of PRODAN (3.5  $\mu$ M) was prepared. Different amounts of  $\alpha$ - and  $\gamma$ -CD were then dissolved in the prepared solution to give the following CD concentrations:  $\sim 5.3 \times 10^{-4}$  M (solution 1),  $\sim 1.0 \times 10^{-3}$  M (solution 2),  $\sim 5.0 \times 10^{-3}$  M (solution 3), and  $\sim 2.0 \times 10^{-2}$  M (solution 4).

The situation is slightly different for the case of  $\beta$ -CD since the maximum solubility of the CD in water is about  $1.5 \times 10^{-2}$  M. This means only solution 4 (only for  $\beta$ -CD aqueous solution) possesses this concentration. Solutions 1, 2, and 3 have the same concentrations as their  $\alpha$ - and  $\gamma$ -CD analogues.

### Temperature Variation System

For the purpose of temperature variation, a temperature controller and circulator (Model RTE-101, Neslab Instrument, Inc.) was employed.

## Spectral Measurements

### Emission Spectra

The fluorescence spectra were collected using an Edinburgh Analytical Instruments Model FS-900CDT spectrofluorometer. It consists of six major components as shown in Fig. 1 and described in the following paragraphs.

*Light Source.* A xenon, high-pressure, arc lamp of 450-W power run from an electrically stabilized d.c. power supply is used as the light source. The lamp housing is optically designed to focus the image of the lamp arc into the entrance slit of the excitation monochromator.

The power unit includes an automatic electronic lamp ignition and lamp temperature monitoring systems.

*Excitation Monochromator.* A  $\frac{1}{3}$ -m-focal length, Czerny–Turner type is used as the excitation monochromator. It is fitted with 1800 g/mm holographic diffraction grating, blazed at 250 nm. The slits are manually adjusted from 10  $\mu$ m to 10 mm, enabling a spectral resolution range of 0.01–9 nm. Wavelength selection, scanning, and wavelength readout are fully controlled by a microprocessor via an IEEE communication protocol.

*Emission Monochromator.* The construction of the emission monochromator is similar to the one used for the selection of the excitation wavelength, except for the diffraction grating, which is ruled and blazed at 500 nm.

*Sample Chamber.* The cell housing is arranged for L or T geometry configurations. It is fitted with a liquid-thermostated, computer-controlled, three-position cell holder unit. An external liquid circulator, cooler/heater, is connected to the cell holders via rubber hoses. The cooling/heating liquid is normally water mixed with ethylene glycol. By controlling the percentage of the water/ethylene glycol mixture, a temperature range of  $-25$ – $85^\circ\text{C}$  can be easily achieved.

*Detection System.* A Hamamatsu photomultiplier tube (PMT), Model IP-28, is used as the photodetector. It is fitted into a thermoelectrically cooled housing (Peltier cooler) to minimize the dark current. The PMT temperature is adjusted to  $-20^\circ\text{C}$ , causing a reduction in the dark current to around 5 counts/s. The PMT output is fed into a 16-bit analog-to-digital converter (ADC). The maximum current that can be drawn from the PMT corresponds to 65,000 ADC counts. During all our spectral measurements, the monochromator slits were fixed to a 50- $\mu$ m width, enabling a spectral resolution of 0.05 nm and a maximum intensity of less than 20,000 counts, corresponding to one-third of the PMT saturation limit.

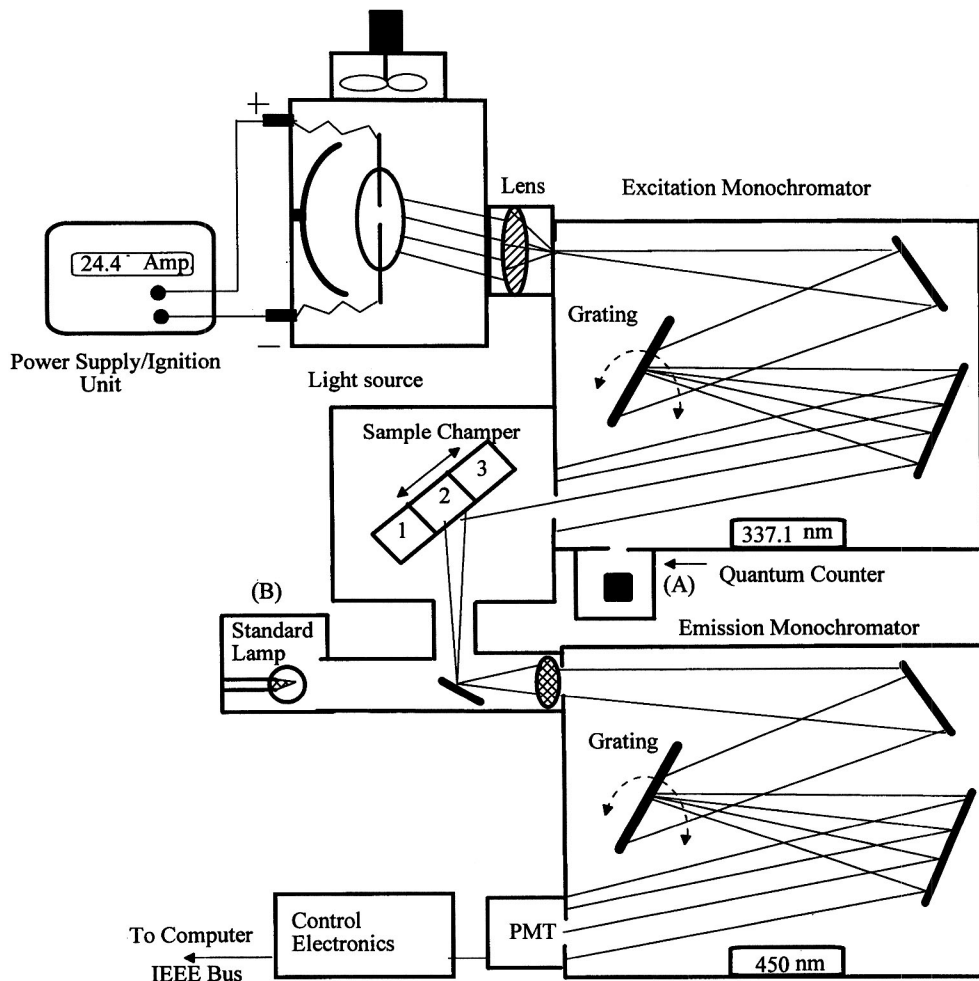


Fig. 1. Simplified diagram of the Model FS-900CDT fluorescence spectrometer.

It is connected to an external water circulator in order to dissipate the heat absorbed by the Peltier cooler.

**System Control and Data Station.** A 486 DX-II/66-MHz PC, supporting a GEM/3 environment, is interfaced to the system via an IEEE interface bus. The software/hardware interface enables the complete control of the system including all the options such as the selection of cells, the readout of cells temperature, and the selection of polarizers. In addition, the software enables data manipulation such as background subtraction, normalization, multiscans, . . . , etc.

**Excitation and Emission Spectral Correction Units.** With the aid of the computer, all spectra are automatically corrected for the wavelength response of the excitation source or the detection units using prestored data files.

A rhodamine B quantum counter (marked A in Fig. 1) is used to measure the spectral irradiance of the excitation source together with the efficiency of the excitation monochromator.

A 10-W tungsten halogen frosted bulb (marked B in Fig. 1) in combination with a highly stable constant power supply is used to correct for the wavelength dependence of the emission monochromator and PMT. It covers a usable range between 250 and 3000 nm.

#### Fluorescence Lifetime Measurements

Fluorescence decay lifetimes measurements were obtained by the technique of time-correlated single-photon counting using an Edinburgh Instrument 199M [20].

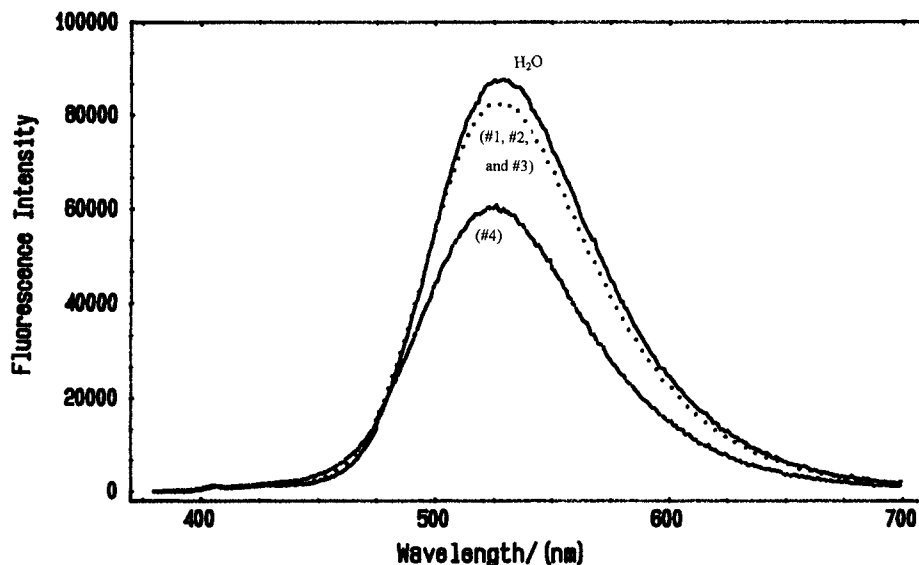


Fig. 2. Fluorescence spectra of  $3.5 \times 10^{-6} M$  PRODAN in water (—) ( $H_2O$ ) and in  $\alpha$ -CD aqueous solutions of different concentrations:  $5.3 \times 10^{-4}$ ,  $1.0 \times 10^{-3}$ , and  $5.0 \times 10^{-3} M$  (.....) (#1, #2, and #3) and (— · — · — ·)  $2.0 \times 10^{-2} M$  (#4); at room temperature.  $\lambda_{exc} = 350$  nm.

## RESULTS

PRODAN is a hydrophobic molecule that is sparingly soluble in water, making PRODAN-saturated solutions possess a concentration of only about  $3.5 \mu M$ . This limited solubility is reflected on the obtained absorption bands of PRODAN in water as well as in CD aqueous solutions, i.e., a very very low-intensity band. The situation is clear, however, for steady-state fluorescence measurements performed at room temperature employing an excitation wavelength of 350 nm.

For  $\alpha$ -CD aqueous solutions, the fluorescence emission of PRODAN is only slightly affected by increasing the CD concentration from 0 to about  $2.0 \times 10^{-2} M$  ( $\lambda_{em} = 527$  nm) as shown in Fig. 2, leading us to say that PRODAN has the same spectral behavior in  $\alpha$ -CD aqueous solutions that it does in water. In  $\beta$ -CD aqueous solutions, however, a blue shift of  $\sim 560$   $cm^{-1}$  accompanied by broadening at the blue edge of the fluorescence band is observed (as shown in Fig. 3) upon increasing the  $\beta$ -CD concentration from 0 ( $\lambda_{em} = 530$  nm) to  $\sim 1.5 \times 10^{-2} M$  ( $\lambda_{em} = 527$  nm).

In  $\gamma$ -CD aqueous solutions, dramatic changes occur as shown in Fig. 4. For the freshly prepared samples, increasing the  $\gamma$ -CD concentration from 0 to  $2.0 \times 10^{-2} M$  is accompanied by a blue shift ( $\lambda_{Fl}$  changes from 527 to 515 nm) and band broadening, compared to both  $\alpha$ - and  $\beta$ -CD aqueous solutions. Especially for solution 4,

a clear shoulder appears in the blue region ( $\sim 435$  nm) of the band.

The situation becomes more clear as time proceeds, and when equilibrium is accomplished. Figure 5 shows how the mentioned shoulder (in Fig. 2) becomes a band while the initially observed band almost disappears. The mentioned equilibrium appears clearly in Fig. 5, which represents the time-dependent emission of PRODAN in  $\gamma$ -CD aqueous solution 4. Actually about 3 months was needed to reach the described equilibrium. For the cases of PRODAN in  $\alpha$ - and  $\beta$ -CD, time shows no appreciable effect.

Figure 6 demonstrates the temperature effect on the emission of PRODAN in  $\gamma$ -CD aqueous solution 4, which has already reached equilibrium. Upon increasing the temperature from  $-12$  to  $75^\circ C$ , the 435-nm peak is depressed while the 510-nm band rises. However, decreasing the temperature again to  $25^\circ C$  fails to bring the system back to the mentioned equilibrium, as shown in Fig. 7

Fluorescence decay lifetimes were calculated for all the studied solutions by using a biexponential fit model. Figure 8 shows that the fluorescence decay curves of PRODAN in water and in  $\alpha$ -CD aqueous solution 4 are indistinguishable. The corresponding fluorescence decay lifetimes are listed in Table I. In  $\beta$ -CD aqueous solutions, the situation is quite different as shown in Fig. 9, which shows different fluorescence decay curves of

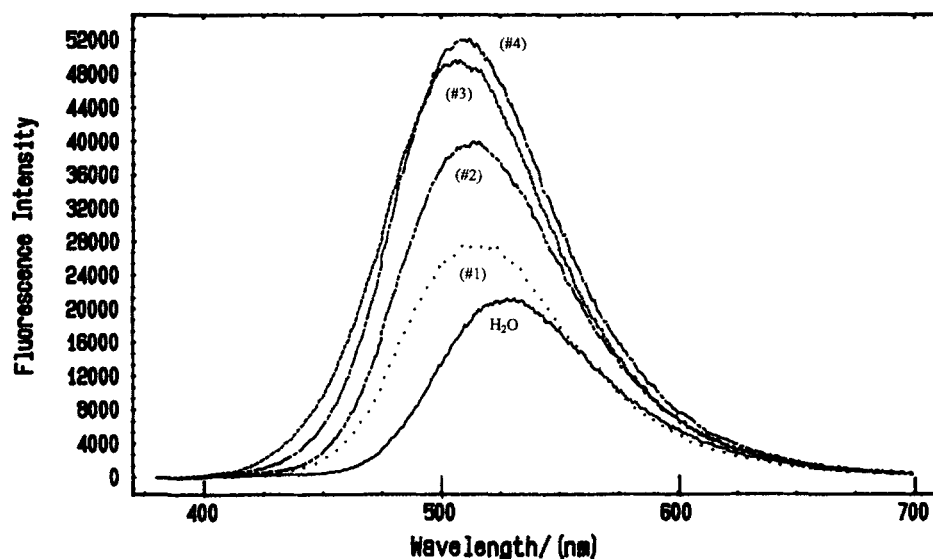


Fig. 3. Fluorescence spectra of  $3.5 \times 10^{-6} M$  PRODAN in water (—) ( $H_2O$ ) and in  $\beta$ -CD aqueous solutions of different concentrations: (.....)  $5.3 \times 10^{-4} M$  (#1), (— — —)  $1.0 \times 10^{-3} M$  (#2), (— — — —)  $5.0 \times 10^{-3} M$  (#3); and (— · — · —)  $1.5 \times 10^{-2} M$  (#4), at room temperature.  $\lambda_{Exc} = 350$  nm.

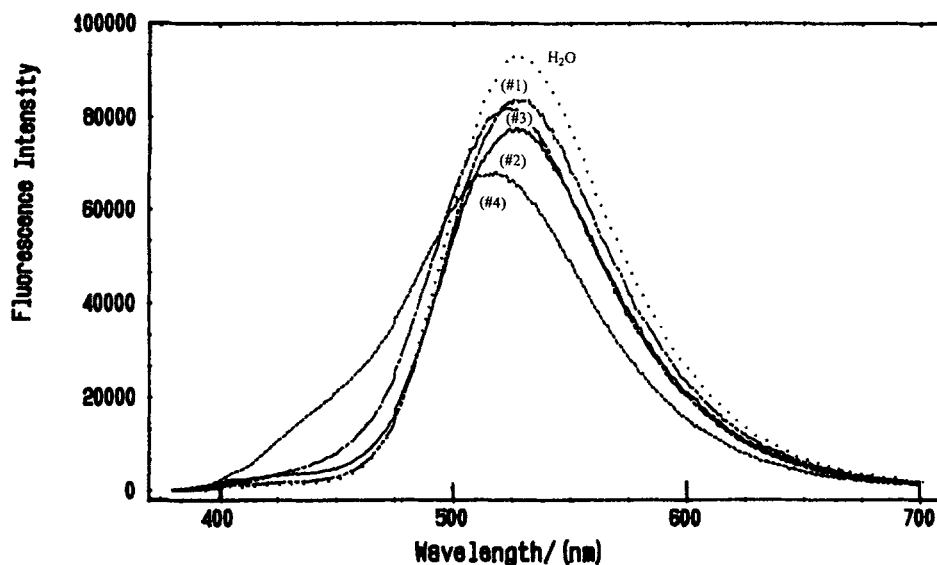


Fig. 4. Fluorescence spectra of  $3.5 \times 10^{-6} M$  PRODAN in water (.....) ( $H_2O$ ) and in  $\gamma$ -CD aqueous solutions of different concentrations: (— · — · —)  $5.3 \times 10^{-4} M$  (#1), (— — —)  $1.0 \times 10^{-3} M$  (#2), (— — — —)  $5.0 \times 10^{-3} M$  (#3), and (— — — —)  $2.0 \times 10^{-2} M$  (#4), at room temperature.  $\lambda_{Exc} = 350$  nm.

PRODAN in water and in  $\beta$ -CD aqueous solution 4. Their corresponding fluorescence decay lifetimes are listed in Table II. From Table II, it is clear that the contribution of the long-lived component ( $\tau_2$ ) increases with increasing concentration of  $\beta$ -CD in PRODAN aqueous solutions.

The fluorescence decays of PRODAN in  $\gamma$ -CD aqueous solution 4 monitored at 435 and at 510 nm are shown in Fig. 10. Their corresponding lifetimes compared to water are listed in Table III. The mean lifetime is found to be longer on going from the less polar (435-nm) state to the more polar (510-nm) state.

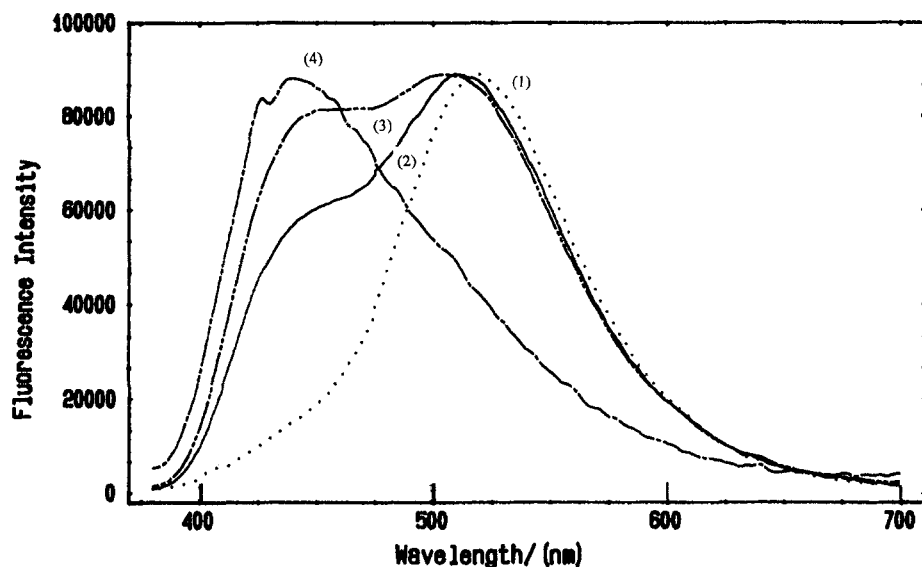


Fig. 5. Fluorescence spectra (normalized) of  $3.5 \times 10^{-6} M$  PRODAN in  $2.0 \times 10^{-2} M$  aqueous solutions of  $\gamma$ -CD (solution 4) (.....) freshly prepared (1), (—) after 10 min (2), (---) after 25 h (3), and (— · — · —) after 3 months (at equilibrium) (4), at room temperature.  $\lambda_{\text{Exc}} = 350 \text{ nm}$ .

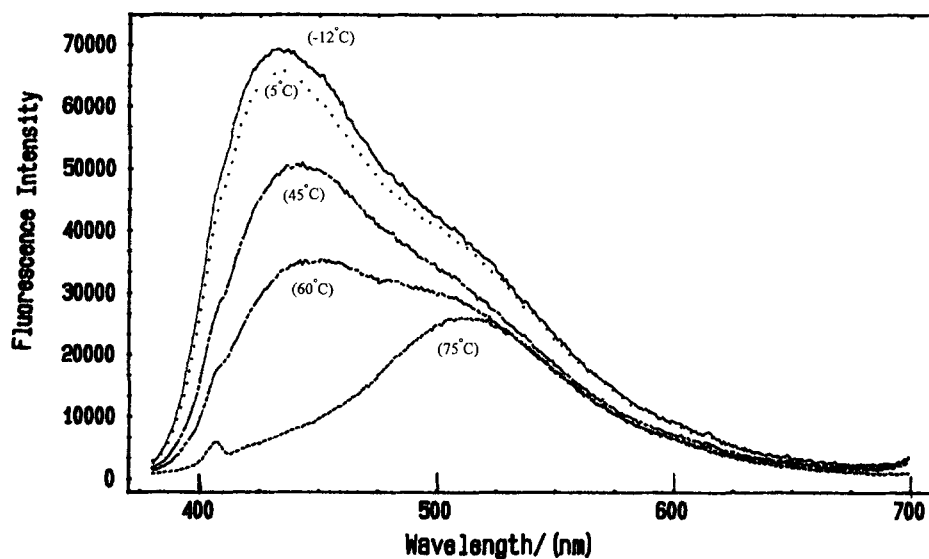


Fig. 6. Effect of increasing temperature on the fluorescence of  $3.5 \times 10^{-6} M$  PRODAN in  $2.0 \times 10^{-2} M$  aqueous solutions of  $\gamma$ -CD (already at equilibrium): (—)  $-12^\circ\text{C}$ , (.....)  $5^\circ\text{C}$ , (---)  $45^\circ\text{C}$ , (— · — · —)  $60^\circ\text{C}$ , and (— · — · —)  $75^\circ\text{C}$ .  $\lambda_{\text{Exc}} = 350 \text{ nm}$ .

Table IV shows the effect of increasing the temperature from  $-15$  to  $20^\circ\text{C}$  on the fluorescence decay of PRODAN in  $\gamma$ -CD aqueous solution 4. The mean lifetime of the less polar state at  $435 \text{ nm}$  is nearly unaffected by the elevation of temperature ( $\tau_f$  changed from  $3.6$  to

$3.5 \text{ ns}$  upon increasing the temperature from  $-15$  to  $20^\circ\text{C}$ ). The corresponding change in the mean lifetime of the more polar state at  $510 \text{ nm}$  is, however, greater. It decreases from  $4.6$  to  $3.8$  upon increasing the temperature from  $-15$  to  $20^\circ\text{C}$ .



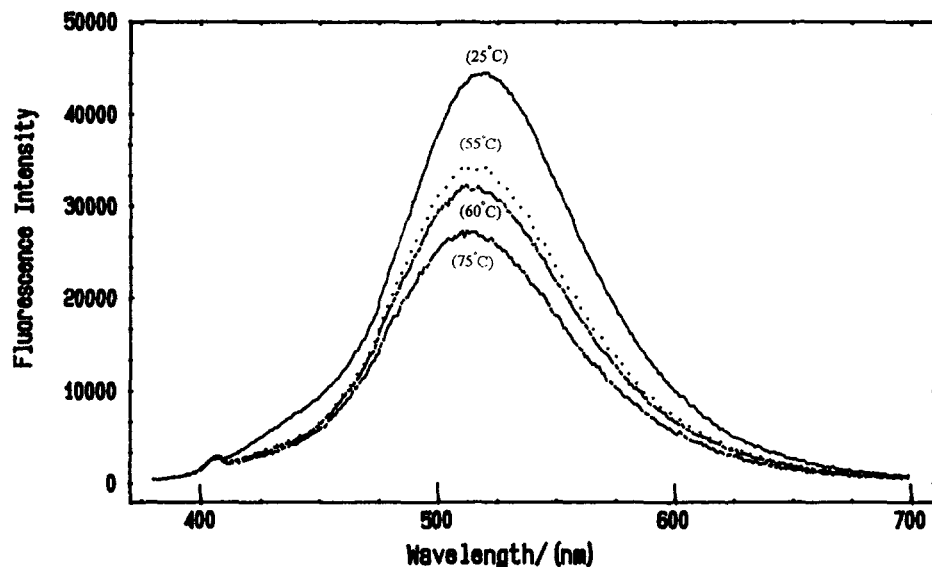


Fig. 7. Effect of decreasing temperature on the fluorescence of  $3.5 \times 10^{-6} M$  PRODAN in  $2.0 \times 10^{-2} M$  aqueous solutions of  $\gamma$ -CD (solution 4) after being heated to (from Fig. 5.) (---) 75°C, (-·-·-) 60°C, (·····) 55°C, and (—) 25°C.  $\lambda_{\text{Exc}} = 350 \text{ nm}$ .

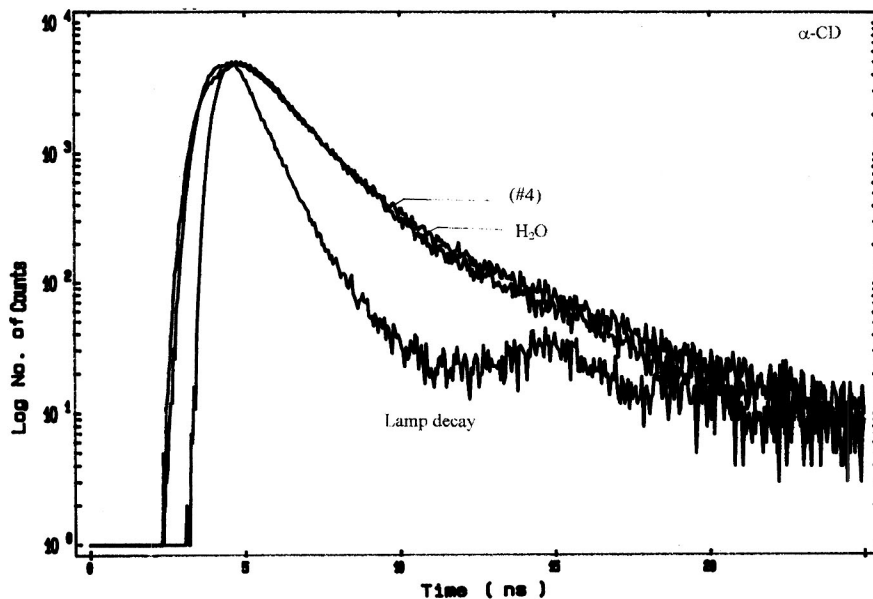


Fig. 8. Fluorescence decay curves of  $3.5 \times 10^{-6} M$  PRODAN in water ( $\text{H}_2\text{O}$ ) and in  $2.0 \times 10^{-2} M$   $\alpha$ -CD aqueous solution 4, at room temperature.  $\lambda_{\text{Exc}} = 358 \text{ nm}$ .

## DISCUSSION

As shown in Fig. 2, the fluorescence emission of PRODAN in  $\alpha$ -CD aqueous solutions is similar to that of PRODAN in water. This observation indicates the

absence of inclusion complexation between the probe and the  $\alpha$ -CD. The observed depression in the fluorescence band in the case of solution 4 compared to the related solutions can be explained by considering hydrogen-bonding between PRODAN and the secondary hy-

**Table I.** Fluorescence Decay Lifetimes of PRODAN in  $\alpha$ -Cyclodextrin Aqueous Solutions

Solution number	$\lambda_{Exc}$ (nm)	$\lambda_{Em}$ (nm)	$\tau_1$ (ns)	$Q_1$	$\tau_2$ (ns)	$Q_2$	$\chi^2$	$\tau_{mean}$ (ns)
PRODAN								
in water	358	530	0.53	0.55	2.0	0.45	1.2	1.2
Solution 1	358	530	0.70	0.68	2.5	0.32	1.0	1.3
Solution 2	358	530	1.1	0.75	2.2	0.25	1.3	1.4
Solution 3	358	530	0.94	0.65	2.6	0.35	1.1	1.5
Solution 4	358	530	0.80	0.59	2.7	0.41	1.0	1.7

droxyl groups of the CD [9]. This interaction is unfavored by the hydrophobic probe, causing the noticed depression.

The absence of inclusion complexation is supported by the fluorescence decay lifetime measurements represented in Fig. 8 and Table I; i.e., the corresponding mean lifetime is almost unaffected by the addition of  $\alpha$ -CD.

For PRODAN in  $\gamma$ -CD, for the freshly prepared sample, the initial local fluorescence maximum at about 510 nm is referred to the formation of an inclusion complex between PRODAN and  $\gamma$ -CD where the dimethylamino group is headed toward the larger rim of the  $\gamma$ -CD cavity. Here, PRODAN senses a relatively slightly polar and slightly rigid environment. The produced complex is usually named type I complex, as shown in Fig. 11.

As time proceeds, the occupied cups—type I complexes—collide with the empty CD cups, which exist in a very large amount (since the PRODAN-to- $\gamma$ -CD concentration ratio is about 1:10<sup>4</sup>), to yield 2:1 complexes, as shown in Fig. 12. Here, PRODAN molecules inside the initially occupied cups merge slowly inside the second empty cups, with the dimethylamino group headed toward the small rims of the CD cavities, sensing the least polar and most rigid environmental conditions, and a new type of complex is produced, namely, the type II complex. A type II complex is represented in Fig. 11, beside a type I complex.

These environmental changes are reflected in the emission spectra of PRODAN in the  $\gamma$ -CD aqueous solution and appear as a continuous depression in the 510-nm peak, attributed to type I complexes, and a gradual rise of the shoulder to give a new local maximum at about 435 nm, a band attributed to type II complexes (refer to Fig. 5).

The high concentration of CD in relation to the probe permits only a tiny amount of the probe to exist in the polar aqueous bulk, while almost all probes are included in the  $\gamma$ -CD cavities.

A complementary tool helpful in confirming our predictions related to PRODAN in  $\gamma$ -CD is the temperature effect on the emission of the probe in  $\gamma$ -CD solution 4 which has already reached equilibrium. Upon increasing the temperature from  $-12$  to  $75^\circ\text{C}$ , the 435-nm peak is depressed while the 510-nm band rises. However, decreasing the temperature again to  $25^\circ\text{C}$  fails to bring the system back to the mentioned equilibrium; these variations are shown in Figs. 6 and 7. Here a temperature elevation will catalyze the exclusion of PRODAN from the  $\gamma$ -CD cavities. As a consequence, the concentration of type II complexes will decrease sharply, and the easily produced type I complexes will be generated again and become the predominant species. The failure of regeneration of type II complexes upon a sudden decrease in temperature from  $75$  to  $25^\circ\text{C}$  adds more evidence that the desired equilibrium needs an appreciable time interval to be accomplished.

This discussion is in line with the unmatched fluorescence decay lifetimes of PRODAN in  $\gamma$ -CD (solution 4). As shown in Table III, the shorter lifetime,  $\sim 3.5$  ns, is due to PRODAN in  $\gamma$ -CD of type II complexes. In this case the dimethylamino groups are directed toward the smaller rims of  $\gamma$ -cavities (this represents the most rigid and least polar environment). Moreover, we believe that the longer fluorescence decay component of PRODAN in  $\gamma$ -CD aqueous solution 4, monitored at 510 nm, is due to PRODAN- $\gamma$ -CD of type I complexes. In this case, the dimethylamino group is directed toward the larger rims of  $\gamma$ -cavities (this represents the less rigid and more polar environment).

One possible explanation for the enhanced lifetime for the more polar state, compared to the less polar state (according to Balter et al. [5]), is the enhanced intersystem crossing (ISC) from the less polar state to the first triplet state compared to intersystem crossing (ISC) from the more polar state to the same triplet state.

In conclusion, we believe that the more polar state (the 510-nm fluorescence band) is controlled more by the polarity of the medium (that is, polarity is more predominant than local microviscosity). On the other hand, the 435-nm fluorescence band (which represents the less polar state) is controlled by the viscosity of the medium (i.e., local microviscosity is more predominant than local polarity).

This interpretation is confirmed by the temperature effect study on the fluorescence decay of PRODAN in  $\gamma$ -CD aqueous solution 4, in the two mentioned states, the 435- and 510-nm states, which represent the less polar and more polar states, respectively. Table IV shows the effect of increasing the temperature from  $-15$  to

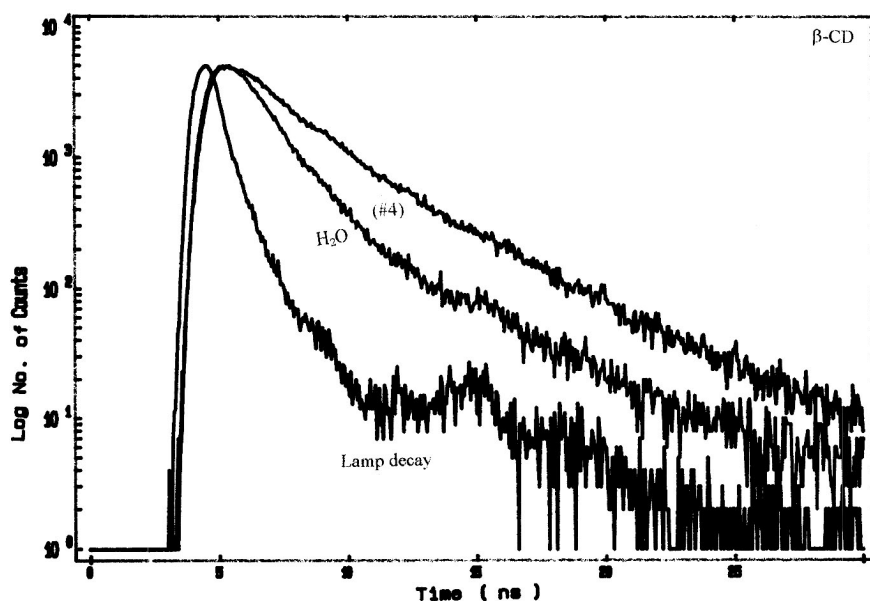


Fig. 9. Fluorescence decay curves of  $3.5 \times 10^{-6} M$  PRODAN in water ( $H_2O$ ) and in  $1.5 \times 10^{-2} M$   $\beta$ -CD aqueous solution 4, at room temperature.  $\lambda_{Exc} = 358$  nm.

Table II. Fluorescence Decay Lifetimes of PRODAN in  $\beta$ -Cyclodextrin Aqueous Solutions

Solution number	$\lambda_{Exc}$ (nm)	$\lambda_{Em}$ (nm)	$\tau_1$ (ns)	$Q_1$	$\tau_2$ (ns)	$Q_2$	$\chi^2$
PRODAN							
in water	358	530	0.53	0.55	2.0	0.45	1.2
Solution 1	358	510	1.1	0.45	3.2	0.55	1.2
Solution 2	358	510	1.4	0.50	3.4	0.50	1.2
Solution 3	358	510	1.2	0.39	3.2	0.61	1.3
Solution 4	358	510	1.4	0.38	3.6	0.62	1.2

20°C on the fluorescence decay of PRODAN in  $\gamma$ -CD aqueous solution 4.

As shown in Table IV, the mean lifetime of the less polar state (the 435-nm emitting state) is almost unaffected by the temperature elevation since the mean lifetime decreases from 3.6 ns at  $-15^\circ C$  to only 3.5 ns at  $20^\circ C$ . This empirical observation agrees with our prediction about the formation of type II complexes, where the PRODAN:  $\gamma$ -CD molecular ratio is 1:2, causing the probe to be encapsulated inside the  $\gamma$ -cavities and moving only inside the channel made by their (the two cups) head-to-head combination. Hence, PRODAN is probably unaffected by external influences, which include the mentioned temperature elevation; as a consequence, the corresponding mean lifetime is also unaltered.

The situation is quite different for the case where PRODAN molecules are included in the  $\gamma$ -cavities, with the dimethylamino group directed toward the larger rims of the  $\gamma$ -cavities, forming type I complexes. As shown in Table IV, the fluorescence decay mean lifetime of PRODAN in  $\gamma$ -CD aqueous solution 4, in the more polar 510-nm state, decreases from 4.6 to 3.8 ns upon increasing the temperature from  $-15$  to  $20^\circ C$ . To explain this experimental trend, the description of type I complexes must be regarded. Here, PRODAN exists inside the  $\gamma$ -cavities with the dimethylamino group directed toward the larger rims of the  $\gamma$ -cavities, sensing a more rigid and less polar environment, with respect to the case where PRODAN molecules exist in the aqueous bulk. Increasing the temperature from  $-15$  to  $20^\circ C$  will catalyze partial expulsion of PRODAN from the  $\gamma$ -cavities, causing the dimethylamino groups to sense relatively more polar and less rigid environmental conditions; as a consequence, the corresponding lifetime will decrease.

For PRODAN in  $\beta$ -CD, the situation is between that in  $\alpha$ -CD and that in  $\gamma$ -CD. Here, the local fluorescence maximum resides at about 515 nm, with an extremely broad band compared with those in the case of  $\alpha$ -CD and without any detected shoulder elsewhere as in the case of PRODAN in  $\gamma$ -CD. This description fits the prediction states that PRODAN in  $\beta$ -CD aqueous solution exists in the form of an inclusion complex, namely, the easily formed type I complex, i.e., with the

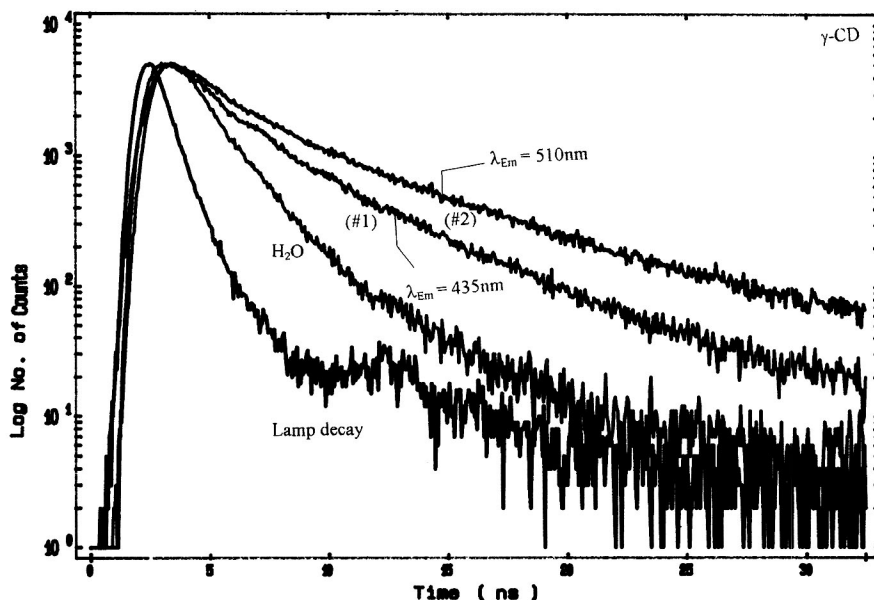


Fig. 10. Fluorescence decay curves of  $3.5 \times 10^{-6} M$  PRODAN in water ( $H_2O$ ) and in  $2.0 \times 10^{-2} M$   $\gamma$ -CD aqueous solutions monitored at 435 nm (#1) and 510 nm (#2), at  $20^\circ C$ .  $\lambda_{Exc} = 358$  nm.

Table III. Fluorescence Decay Lifetimes of PRODAN in  $\gamma$ -Cyclodextrin Aqueous Solution 4

Solution number	$\lambda_{Exc}$ (nm)	$\lambda_{Em}$ (nm)	$\tau_1$ (ns)	$Q_1$	$\tau_2$ (ns)	$Q_2$	$\chi^2$	$\tau_{mean}$ (ns)
PRODAN								
in water	358	530	0.53	0.55	2.00	0.45	1.2	1.2
Solution 4	358	510	0.66	0.36	5.51	0.64	1.2	3.8
Solution 4	358	435	1.33	0.42	5.10	0.58	1.2	3.5

Table IV. Temperature Effect on Fluorescence Decay Lifetimes of PRODAN in  $\gamma$ -Cyclodextrin Aqueous Solution 4

Temperature ( $^\circ C$ )	$\lambda_{Exc}$ (nm)	$\lambda_{Em}$ (nm)	$\tau_1$ (ns)	$Q_1$	$\tau_2$ (ns)	$Q_2$	$\chi^2$	Mean $\tau$ (ns)
-15	358	435	1.88	0.45	4.92	0.55	1.3	3.6
-15	358	510	1.31	0.27	5.85	0.73	1.4	4.6
20	358	435	1.31	0.42	5.10	0.58	1.2	3.5
20	358	510	0.66	0.36	5.51	0.64	1.2	3.8

dimethylamino groups toward the larger rims of  $\beta$ -cavities. The measured fluorescence decay lifetimes (Table II and Fig. 9) of PRODAN in  $\beta$ -CD aqueous solutions indicate the presence of a longer-lived component whose contribution increases with increasing concentration of  $\beta$ -CD. This is an indication of complex formation between PRODAN and  $\beta$ -CD.

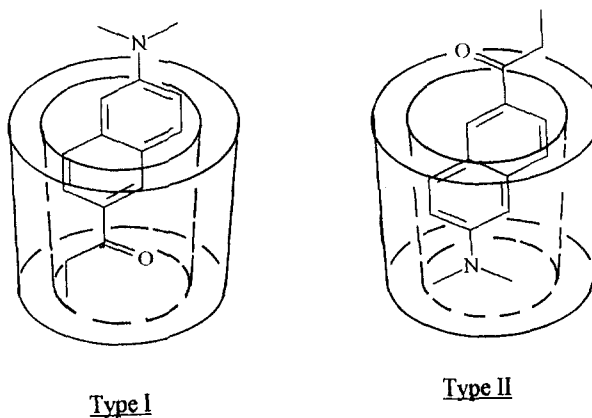


Fig. 11. Possible positions of PRODAN in the  $\gamma$ -CD cavity. type I, dimethylamino group toward the larger rim; and type II, dimethylamino group toward the smaller rim.

In conclusion, it is the direction of the dimethylamino group of PRODAN (toward the smaller rim or toward the large rim of the  $\gamma$ -CD cavity) that governs the generation of two kinds of fluorescence, a less polar,  $\sim 435$  nm (type II complexes) and a more polar,  $\sim 510$  nm (type I complexes), observed for PRODAN in  $\gamma$ -CD aqueous solutions. This is similar to our previous observations made for DMABN in  $\alpha$ -CD aqueous solutions [23]. DMABN in  $\alpha$ -CD aqueous solutions was found to emit two fluorescence bands, at  $\sim 460$  and  $\sim 520$  nm,

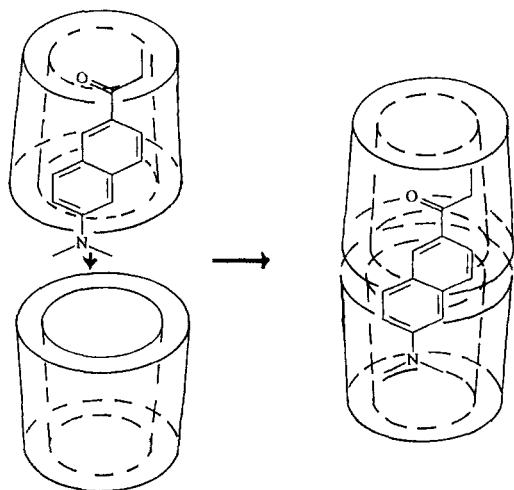


Fig. 12. Possible mechanism for slow formation of type II from type I complexes in the presence of a large amount of  $\gamma$ -CD.

besides the normal B-fluorescence band at  $\sim 345$  nm. These 460- and 520-nm fluorescence bands were attributed to emission from a less polar (type II complexes: the dimethylamino group of DMABN is directed toward the smaller rim of the  $\alpha$ -CD cavity) and from a more polar (type I complexes: the dimethylamino group is directed toward the larger rim of the  $\alpha$ -CD cavity) TICT state (Fig. 5 in Ref. 23). These conclusions were confirmed using excitation spectra and fluorescence decay results. The similarity of the results obtained for PRODAN in  $\gamma$ -CD (see text) to the results obtained previously for DMABN in  $\alpha$ -CD [23] encourages us to place PRODAN on the TICT fluorescence probe list. This leads us to attribute the two fluorescence bands of PRODAN,  $\sim 510$  and  $\sim 435$  nm, in  $\gamma$ -CD aqueous solutions to the twisting of the dimethylamino group in media of different polarities present in the same solution. These media are presented in Fig. 11 as type I and type II complexes. The relative contribution of the two fluorescence bands (observed for PRODAN in  $\gamma$ -CD) at 510 and at 435 nm depends on the concentration of type I and type II complexes, respectively, in the solution. Type I complexes are the dominant ones for freshly prepared samples and type II complexes are more dominant for solutions that have reached equilibrium. Moreover, temperature has a major effect on the concentration of the two types of complexes as mentioned earlier.

To examine the validity of the proposed models for the case of DMABN in  $\alpha$ -CD aqueous solutions, we extended our study to DEABN [24]. DEABN has a larger donor group (the diethylamino group in DEABN is bigger than the dimethylamino group in DMABN) and

behaves in a different manner from DMABN in  $\alpha$ -CD cavities. The less polar TICT fluorescence band at  $\sim 460$  nm was completely absent from DEABN as opposed to DMABN. We attributed that to the large size of the diethylamino group in DEABN, which becomes interlocked in the  $\alpha$ -CD cavity when type II complexes are formed and therefore is unable to rotate during the excited-state lifetime [24]. The 520-nm fluorescence band, however, was observed for the case of DEABN in  $\alpha$ -CD and was attributed to type I complexes, where the diethylamino group is directed toward the larger rim of the  $\alpha$ -CD cavity and has the freedom to rotate during the excited-state lifetime. These results and interpretation were also confirmed by the excitation spectra and fluorescence decay results.

Finally, it is our concern to investigate further the effect of  $\gamma$ -CD cavity size on the emission characteristics of some molecules related to PRODAN in a fashion similar to that used to study DMABN and DEABN in  $\alpha$ -CD aqueous solutions. Then we will be able to judge the validity of the proposed model concerning PRODAN fluorescence in  $\gamma$ -CD cavities.

## ACKNOWLEDGMENTS

The FS900 CDT spectrofluorometer and the photon counting setup (Edinburgh Instruments) were fully provided to us by EEC/Europe under the EC/Jordan—Cooperation Project in Science and Technology (SEM/03/628/033)—Polymer Project. Their support is greatly appreciated. Our thanks extend to our colleague Dr. Yaser A. Yousef for assistance in measurements of lifetime decays and for the useful discussion. Our thanks also go to Dr. T. Azumi (Tohoku University) for the supply of PRODAN and cyclodextrins.

## REFERENCES

1. G. Weber and F. G. Farris (1979) *Biochemistry* **18**, 3075.
2. P. Avouris, W. M. Gelbert, and M. A. El-Sayed (1977) *Chem. Rev.* **77**, 793.
3. J. R. Lackowicz and A. Balter (1982) *Biophys. Chem.* **16**, 117.
4. W. Nowak, P. Adamczak, A. Balter, and A. Sygula (1986) *J. Mol. Struct. (Theochem.)* **13**, 139.
5. A. Balter, W. Nowak, W. Pawelkiewicz, and A. Kowalczyk (1988) *Chem. Phys. Lett.* **143**, 565.
6. P. L. G. Chong (1988) *Biochemistry* **27**, 399.
7. A. Sommer, F. Baltauf, and A. Hermetter (1990) *Biochemistry* **29**, 11134.
8. J. Zeng and P. L. G. Chong (1991) *Biochemistry* **30**, 9485.
9. H. Rottenberg (1992) *Biochemistry* **31**, 9473.
10. U. Narang, J. D. Jordan, F. V. Bright, and P. N. Prasad, (1994) *J. Phys. Chem.* **89**, 8101.

11. E. Lippert, W. Luder, and H. Boss (1962) in A. Mangini (Ed.), *Advances in Molecular Spectroscopy*, Pergamon Press, Oxford.
12. G. Wermuth and W. Rettig (1984) *J. Phys. Chem.* **88**, 2729.
13. J. Lipinski, H. Chojnacki, Z. R. Grabowski, and K. Rotkiewicz (1980) *Chem. Phys. Lett.* **70**, 449.
14. A. M. Rollinson and H. G. Drickamer (1980) *J. Chem. Phys.* **73**, 5981.
15. P. Ilich and F. G. Prendergast (1989) *J. Phys. Chem.* **93**, 4441.
16. F. Heisel, J. A. Miehe, and A. W. Szemik (1987) *Chem. Phys. Lett.* **138**(4), 321.
17. C. E. Bunker, T. L. Bowen, and Y. Sun (1993) *Photochem. Photobiol.* **58**(4), 499.
18. W. Rettig (1986) *Angew. Chem. Int. Ed. Engl.* **25**, 971.
19. K. A. Al-Hassan and W. Rettig (1986) *Chem. Phys. Lett.* **126**, 273.
20. K. A. Al-Hassan and T. Azumi. (1989) *Chem. Phys. Lett.* **129**, 163.
21. R. Hayashi, S. Tazuke, and C. W. Frank (1987) *Chem. Phys. Lett.* **135**, 123; (1987) *Macromolecules* **20**, 983.
22. K. A. Al-Hassan, M. A. Meentani, and Z. F. M. Said (1998) *J. Fluoresc.* (in press).
23. K. A. Al-Hassan, U. K. A. Klein, and A. Suwaiyan, (1993) *Chem. Phys. Lett.* **212**, 581.
24. K. A. Al-Hassan (1994) *Chem. Phys. Lett.* **227**, 527.
25. K. A. Al-Hassan, A. Suwaiyan, and U. K. A. Klein (1997) *Arab. J. Sci. Eng.* **22**, 45-55.
26. A. C. R. Villiers (1891) *Acad. Sci. Paris* 539.
27. F. Schardinger and Z. Untere (1903) *Nahrungs-Genussmittel Gebrauchsgegenstände* **6**, 865.
28. H. Bender (1978) *Carbohydr. Res.* **65**, 85.
29. D. D. MacNicol, J. J. Mckendrick, and D. R. Wilson (1978) *Chem. Soc. Rev.* **7**, 65.